Azimuthal distributions in heavy ion collisions and the nuclear equation of state

G. M. Welke, M. Prakash, T. T. S. Kuo, and S. Das Gupta*
Physics Department, State University of New York at Stony Brook, Stony Brook, New York 11794

C. Gale
Atomic Energy of Canada, Ltd., Chalk River Nuclear Laboratories, Theoretical Physics Branch, Chalk River, Ontario, Canada K0J 1J0
(Received 28 April 1988)

For near central collisions of Nb on Nb at a laboratory energy of 650 MeV per projectile nucleon we calculate inclusive cross sections as a function of the azimuthal angle where this angle is measured from the reaction plane. The azimuthal dependence is strongly influenced by the nuclear equation of state and is a useful quantity to measure.

I. INTRODUCTION

A major goal of heavy-ion collision experiments is to extract information about the nuclear equation of state. One needs to select observables which are influenced by the nuclear equation of state as opposed to those influenced mostly by kinematics, nucleon-nucleon scattering cross sections, geometry, etc. Various observables have been proposed in the past, including pion production,[1] kaon production,[2] flow angles,[3] transverse momenta,[4,5] etc. A summary of the experimental situation and details of models which attempt to calculate these observables can be found in recent review articles.[2,6–8] We also refer the reader to a recent update by Danielewicz.[9]

In this paper we examine azimuthal distributions as a testing ground for the nuclear equation of state. The exact meaning of azimuthal distribution is described in Sec. II. Azimuthal distributions of charged particles have been measured previously.[10] An experiment to measure such distributions for neutrons has been proposed[11] and will be performed at the Bevalac in the near future. Here we report on calculations of azimuthal distributions for collisions of Nb on Nb. It is found that the anisotropy of the azimuthal distributions depends quite strongly on the equation of state used. We also investigate the dependence of the azimuthal distribution on nucleon-nucleon scattering cross sections and find it to be somewhat weak although this may be particular to the example we chose to work with. At the end we shall predict a value for the maximum azimuthal anisotropy.

The fact that the azimuthal distribution is influenced by the nuclear equation of state was pointed out in Ref. 2 (see Fig. 8.4 in that Reference). In calculational details there are major differences between our approach and the near analytical methods used in that paper.

II. AZIMUTHAL DISTRIBUTIONS

Consider a collision of two heavy ions. For nonzero impact parameter b, the beam ($\hat{z}$) direction and the line joining the centers of the nuclei define the reaction plane. This plane is, of course, known *a priori* in a simulation of the collision; we choose it to coincide with the $y=0$ plane and measure azimuthal angles with respect to it. Suppose that before collision nucleus 1 (2) was moving in the positive (negative) z direction with its center at $x=b/2(-b/2)$. In the course of the reaction nucleons from nucleus 1 (2) acquire a net momentum in the positive (negative) x direction (while maintaining overall reflection symmetry about the reaction plane). This property allows one to determine, experimentally, the reaction plane in a given event.[9] Since, however, not all particles are identified and momentum analyzed, estimates of the azimuthal angle of the reaction plane ϕ_R have a nonzero dispersion.[4]

In the transverse momentum method[4,9] one defines for each event a vector $\mathbf{Q}=\sum_i \omega_i \mathbf{p}_\perp(i)$ where i is the particle index and $\omega_i=\mathrm{sgn}(p_z)$; $\mathbf{p}(i)$ is the momentum in the center-of-mass (c.m.) system of the nuclei. The vector $\mathbf{Q}$ then defines the estimated x direction.

In the proposed experiment[11] the reaction plane is to be determined by measuring the transverse velocity of charged particles, $\mathbf{v}_\perp(i)$. The vector[12]

$$\mathbf{V}(y_c)=\sum_i \epsilon(y_i)\theta(y_i-y_c)\omega(v_\perp)\mathbf{v}_\perp(i)\ , \tag{2.1}$$

where

$$\epsilon(y_i)=-\mathrm{sgn}(y_i)$$

and y_i is the rapidity of particle i in the c.m. system, gives the required estimate ϕ_R. y_c denotes a cut in c.m. rapidity and $\omega(v_\perp)$ is a weight factor chosen to minimize dispersion in the reaction plane azimuth.[12] The experiment proposes to measure triple differential cross sections of neutrons and, in particular, the angular dependence of $d\sigma/d(\phi-\phi_R)$. Although inclusive neutron cross sections are harder to measure than proton inclusive cross sections, they were, nevertheless, measured successfully in the past.[13]

The objective of this paper is to examine the sensitivity of $d\sigma/d\phi$ to the nuclear equation of state (EOS). We have performed calculations for Nb on Nb collisions at a laboratory beam energy of 650 MeV/nucleon. The results are integrated over an impact parameter range

chosen with the above experiment in mind.[11] A multiplicity gate allows one to choose the impact parameter range in the experiment.[5] Since projectile and targetlike fragments have a net flow in opposite x directions, it is useful to choose one set or the other; for greater sensitivity to the EOS further cuts may be needed. This is discussed in Sec. III. With our choice of initial conditions and cuts, the maximum $d\sigma/d\phi$ is at $\phi=0°$ and the minimum at $\phi=180°$. We call

$$\mathcal{R}=\frac{(d\sigma/d\phi)_{\max}}{(d\sigma/d\phi)_{\min}} \tag{2.2}$$

to be the maximum azimuthal anisotropy. The quantity $\mathcal{R}$ is related to transverse momenta, but gives some complementary information as it relates p_x to $|p_y|$ (the average value $\langle p_y \rangle$ is of course zero) although it provides no information about the magnitudes of p_x and p_y individually. The in-plane transverse momentum experiments give the magnitude of p_x, but say nothing about $|p_y|$.

In the past it has been difficult to fold into theoretical calculations the effects of acceptance filters in transverse momentum experiments. We do not foresee such difficulties for the azimuthal distributions.

The effect on $\mathcal{R}$ of a finite rms dispersion $\Delta\phi_R$ of the reaction plane may be estimated using a simple form for the azimuthal nucleon inclusive cross section,

$$\frac{d\sigma}{d(\phi-\phi_R)}=a+b\cos(\phi-\phi_R)\ , \tag{2.3}$$

where a and b are suitably defined constants. Assuming a Gaussian distribution for ϕ_R with $\langle \phi_R \rangle=0°$, viz.,

$$n(\phi_R)=\frac{1}{\Delta\phi_R\sqrt{2\pi}}e^{-\phi_R^2/[2(\Delta\phi_R)^2]} \tag{2.4}$$

and $\frac{1}{2}(\pi/\Delta\phi_R)^2 \gg 1$, we then obtain the estimate

$$\mathcal{R}_{\rm est}=\frac{a+be^{-\frac{1}{2}(\Delta\phi_R)^2}}{a-be^{-\frac{1}{2}(\Delta\phi_R)^2}}\ , \tag{2.5}$$

which reduces $\mathcal{R}=(a+b)/(a-b)$ if the reaction plane is exactly determined in each event. Typically, $\mathcal{R}$ is found to be decreased by about 25% for a dispersion of 35°. In the following discussion we assume $\Delta\phi_R=0°$ and choose $\phi_R=0°$.

III. CHOICE OF CUTS IN THE SIMULATION

The calculations performed here use the Boltzmann-Uheling-Uhlenbeck (BUU) formalism which is well documented.[8] The time evolution of the Wigner function $f(\mathbf{r},\mathbf{p},t)$ in phase space is given by

$$\frac{\partial f}{\partial t}+\mathbf{v}\cdot\nabla_r f-\nabla_r U\cdot\nabla_p f=-\frac{1}{(2\pi)^6}\int d^3p_2 d^3p_{2'} d\Omega \frac{d\sigma_{NN}}{d\Omega} v_{12}$$
$$\times\{[ff_2(1-f_{1'})(1-f_{2'})-f_{1'}f_{2'}(1-f)(1-f_2)](2\pi)^3\delta^3(\mathbf{p}+\mathbf{p}_2-\mathbf{p}_{1'}-\mathbf{p}_{2'})\}\ , \tag{3.1}$$

where $d\sigma_{NN}/d\Omega$ and v_{12} are the cross section (energy dependent) and the relative velocity for the colliding nucleons, respectively, and U is the mean-field potential.

In our numerical calculations, we use 60 test particles per nucleon, a grid size of 1.5 fm^3 and a time step of 0.3 fm/c. The impact parameter is averaged over the range $0.4R \le b \le 0.8R$, where the radius R of ^{93}Nb is taken to be $1.14A^{1/3}$ fm. The calculations were done in the c.m. frame. Spectators are defined as particles moving with $0.79 \le |(y/y_p)_{\rm c.m.}| \le 1.11$ (compare with Ref. 14) and in the angular range $0° \le \theta \le 5°$ (or $175° \le \theta \le 180°$), and are ignored. We next consider various laboratory frame rapidity cuts, viz., particles with $(y/y_p)_{\rm lab} > 0.5$ (these would correspond to all participants with momenta $p_z > 0$ in the c.m.) and $(y/y_p)_{\rm lab} > 0.75$. We have also considered participants in the forward direction with $\theta_{\rm lab} < 10°$, $\theta_{\rm lab} < 15°$, and $\theta_{\rm lab} < 20°$. Of all these choices the cut $(y/y_p)_{\rm lab} > 0.75$ is the most profitable in the sense that the maximum azimuthal anisotropy

$$\mathcal{R}=(d\sigma/d\phi)_{0°}/(d\sigma/d\phi)_{180°}$$

is maximum. The ratio $\mathcal{R}$ depends on the equation of state; the harder the equation of state, the higher is the value of $\mathcal{R}$.

IV. DEPENDENCE OF AZIMUTHAL DISTRIBUTIONS ON THE EQUATION OF STATE

In this section we show results with three equations of state. the first one is a soft EOS without any momentum dependence used by Bertsch, Kruse, and Das Gupta (BKD).[15] Here the mean field is given by

$$U(\rho)=-356\left[\frac{\rho}{\rho_0}\right]+303\left[\frac{\rho}{\rho_0}\right]^{7/6}\ (\text{MeV})\ , \tag{4.1}$$

where ρ_0 is the density of cold nuclear matter. The second one is a hard EOS used by BKD for which

$$U(\rho)=-124\left[\frac{\rho}{\rho_0}\right]+70.5\left[\frac{\rho}{\rho_0}\right]^2\ (\text{MeV})\ . \tag{4.2}$$

The third is a momentum dependent interaction used by Gale, Bertsch, and Das Gupta[16] which we shall refer to as the GBD parametrization

$$U(\rho,\mathbf{p}) = -144\left[\frac{\rho}{\rho_0}\right] + 203.3\left[\frac{\rho}{\rho_0}\right]^{7/6} - \frac{75}{\rho_0}\int d^3p \frac{f(\mathbf{r},\mathbf{p})}{1+\left[\frac{\mathbf{p}-\langle\mathbf{p}\rangle}{\Lambda}\right]^2} - \frac{75}{\rho_0}\frac{\rho}{1+\left[\frac{\mathbf{p}-\langle\mathbf{p}\rangle}{\Lambda}\right]^2}\ (\text{MeV}), \quad (4.3)$$

where $\Lambda = 1.5 p_F^{(0)}$. The three equations of state give compression moduli $K = 200$ MeV, 380 MeV, and 215 MeV, respectively. The angular distribution $d\sigma/d\phi$ for the three cases are shown in Figs. 1, 2, and 3. The values of the maximum anisotropy $\mathcal{R}$ are shown in Table I. The BKD soft equation of state gives $\mathcal{R} = 2.0$; the BKD hard EOS gives $\mathcal{R} = 4.3$, and the GBD parametrization gives $\mathcal{R} = 5.2$. The value of $\mathcal{R}$ is sufficiently different for the soft and the hard equations of state that $\mathcal{R}$ is a useful quantity to measure. Not unexpectedly, the momentum dependent GBD parametrization gives a high value of $\mathcal{R}$ despite a compression modulus which is nearly the same as that of the BKD soft equation of state. We shall have more to say about momentum dependent interactions later. In Fig. 4, we show the azimuthal distribution obtained by imposing a cut in the laboratory angle as opposed to a cut in rapidity.

It is necessary to ascertain how sensitive this azimuthal anisotropy is with respect to nucleon-nucleon cross sections. Figures 1 through 4 show the results of calculations using free nucleon-nucleon cross sections σ_{NN}. In-medium corrections will alter these values. Some of this, of course, is taken into account by the Pauli blocking in the BUU formalism. Bertsch *et al.*[17] have considered the effects of reducing the cross sections. More recently,

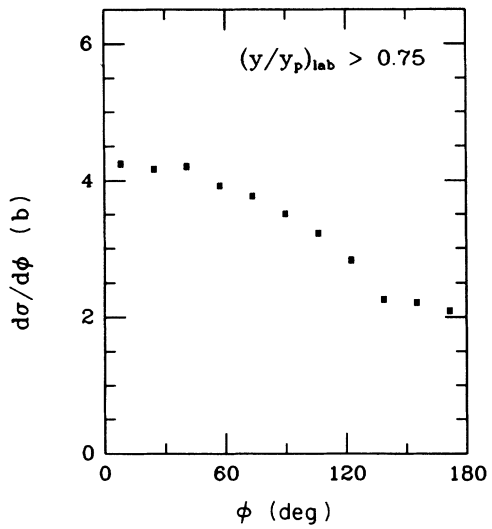

FIG. 1. The azimuthal differential cross section for nucleons, integrated over the impact parameter range $0.4R \le b \le 0.8R$, for Nb + Nb collisions at $E_{\text{lab}}/A = 650$ MeV. A soft BKD interaction is used. The cut in rapidity is displayed.

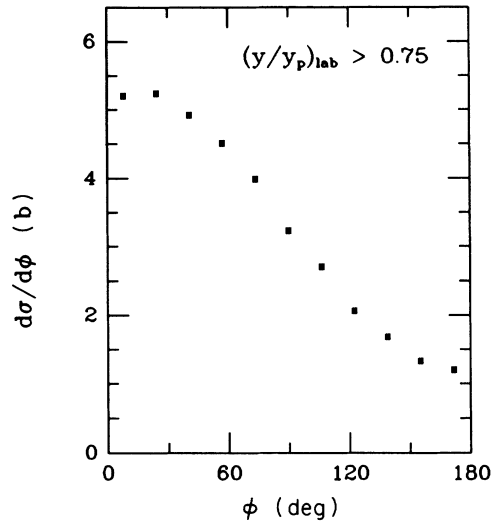

FIG. 2. Same as in Fig. 1, but for the hard BKD interaction.

Bertsch *et al.*[18] have argued that inelastic cross sections should increase with increasing density. We have not changed the cross sections for each of the three equations of states; for the BKD soft EOS we used $\sigma_{\text{med}}/\sigma_{NN} = 1.7$ (both for elastic and inelastic). The results are shown in Fig. 5. The ratio $\mathcal{R}$ changed from 2.0 to 3.0 which is still less than 4.3 (the value for the BKD hard EOS with free nucleon-nucleon cross sections) or 5.2 (the value for the momentum dependent GBD parametrization with free nucleon-nucleon cross sections). We have also performed a calculation with GBD parameters, but with $\sigma_{\text{med}}/\sigma_{NN} = 0.5$ (again both elastic and inelastic). The ratio $\mathcal{R}$ changed from 5.2 to 4.8. These results are summarized in Table I. Thus, in spite of uncertainties in the values of "correct" cross sections, azimuthal anisotropies, at least in this particular case, are useful to gain information about the nuclear equation of state. The cross section σ for nucleons emitted with $(y/y_p)_{\text{lab}} \ge 0.75$ is

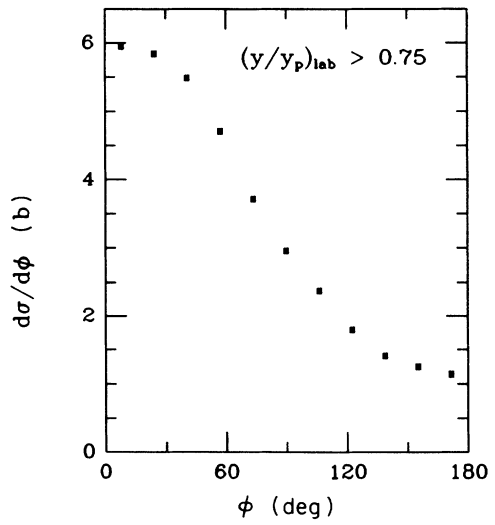

FIG. 3. Same as in Fig. 1, but for the momentum dependent GBD interaction.

TABLE I. Summary of results for Nb on Nb at $E_{lab}/A = 650$ MeV, averaged over an impact parameter range of $0.4R \leq b \leq 0.8R$, where R is the radius of Nb. Column two gives the compression modulus K for the various equations of state. σ_{NN} and σ_{med} refer to the free (Ref. 8) and the in-medium nucleon-nucleon scattering cross sections, respectively. $\mathcal{R}$ and σ are the maximum azimuthal anisotropy and total nucleon cross section, respectively, for particles with lab rapidity $y \geq 0.75 y_p$. The mid-rapidity slope $\tilde{\theta}_F$, the average in-plane transverse momentum $\langle p_x \rangle$ and the maximum flow angle θ_{max} are also given.

EOS	K (MeV)	$\frac{\sigma_{med}}{\sigma_{NN}}$	$\mathcal{R}$	σ (barns)	$\tilde{\theta}_F$ (MeV/c)	$\langle p_x \rangle$ (MeV/c)	θ_{max}
BKD	380	1.0	4.3	21	180	68	14°
BKD	200	1.0	2.0	21	140	47	7°
BKD	200	1.7	3.0	18	200	69	18°
GBD	215	1.0	5.2	21	210	80	16°
GBD	215	0.5	4.8	25	150	64	11°
This work	215	1.0	4.3	21	200	73	15°
This work	380	1.0	7.4	21	240	92	18°

also given in Table I. It is affected only by a change in the nucleon-nucleon scattering cross section.

In Table I, we also show results of other measures of flow, viz., the mid-rapidity slope $\tilde{\theta}_F$ of in-plane transverse momenta $\langle p_x(y/y_p) \rangle$ curves,[5] average in-plane transverse momenta $\langle p_x \rangle$ for particles with $p_x > 0$ in the c.m., and the maximum of a Jacobi-weighted flow angle distribution from sphericity analyses in the c.m. system, θ_{max}.

At the end we would like to quote a predicted value for the ratio $\mathcal{R}$. Since the momentum dependence of the nuclear potential is an established fact, we shall use a momentum dependent potential. However, we shall use a more complicated version than the GBD parametrization. The next section explains why.

V. MOMENTUM DEPENDENCE OF THE EQUATION OF STATE

The GBD parametrization of Eq. (4.3) is simple and adequate provided local equilibrium exists. A recent paper[19] compares $U(\rho, \mathbf{p})$ as given by Eq. (4.3) with the $U(\rho, \mathbf{p})$ derived from the Gogny interaction.[20] The comparison was done for nuclear matter at relevant values of ρ and at zero and 50 MeV temperatures. The numerical values of the potentials are close enough so that the GBD parametrization does an adequate job in most situations.

On closer scrutiny it can be deduced that the two interactions can give quite different results under extreme nonequilibrium situations. Such an extreme nonequilibrium situation will exist for a short time in the early history of a "hit" when the two heavy ions begin to inter-

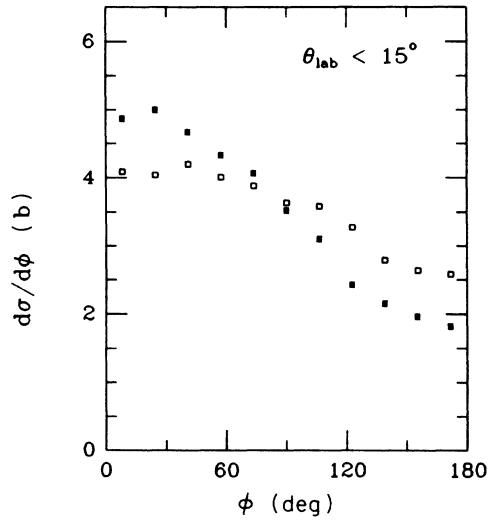

FIG. 4. Azimuthal cross section for participants emitted within a forward cone of 15° in the laboratory frame, with soft (open squares) and hard (solid squares) BKD interactions.

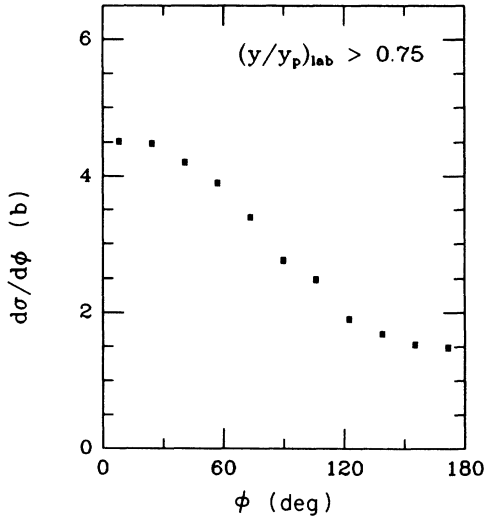

FIG. 5. Same as in Fig. 1, but with the in-medium cross section a factor of 1.7 larger than the free space value.

penetrate and sufficient number of collisions have not yet taken place to degrade the originally directed motion of the two nuclei.

In determinantal theories the exchange terms give rise to a potential energy density

$$V^{\rm ex}=\frac{C'}{\rho_0}\int d^3pd^3p' f(\mathbf{r},\mathbf{p})f(\mathbf{r},\mathbf{p}')g(|\mathbf{p}-\mathbf{p}'|)$$

$$=\frac{C'}{\rho_0}\int d^3pd^3p' \frac{f(\mathbf{r},\mathbf{p})f(\mathbf{r},\mathbf{p}')}{1+\left[\frac{\mathbf{p}-\mathbf{p}'}{\Lambda}\right]^2}, \tag{5.1}$$

where in the last step we have assumed a Yukawa form for $V(|\mathbf{r}-\mathbf{r}'|)$. The Gogny interaction uses a sum of two Gaussians, thus

$$(1+[(\mathbf{p}-\mathbf{p}')/\Lambda]^2)^{-1}$$

would be replaced by $\sum_i e^{-\alpha_i(\mathbf{p}-\mathbf{p}')^2}, i=1,2$. The exact functional form of $V(|\mathbf{r}-\mathbf{r}'|)$ is not crucial so long as the parameters are chosen to fit the binding energy, the compression modulus, the optical potential, etc. We shall stay with the functional form

$$(1+[(\mathbf{p}-\mathbf{p}')/\Lambda]^2)^{-1}$$

as, for our purpose, it is easier to work with. The potential $U_1(\rho,\mathbf{p})$ deduced from $V^{\rm ex}$ [Eq. (5.1)] is easily seen to be

$$U_1(\rho,\mathbf{p})=2\frac{C'}{\rho_0}\int d^3p' \frac{f(\mathbf{r},\mathbf{p}')}{1+\left[\frac{\mathbf{p}-\mathbf{p}'}{\Lambda}\right]^2}. \tag{5.2}$$

This is to be compared with the potential $U_2(\rho,\mathbf{p})$ used in GBD,

$$U_2(\rho,\mathbf{p})=\frac{C}{\rho_0}\int d^3p' \frac{f(\mathbf{r},\mathbf{p})}{1+\left[\frac{\mathbf{p}-\langle\mathbf{p}\rangle}{\Lambda}\right]^2}$$

$$+C\frac{\rho}{\rho_0}\frac{1}{1+\left[\frac{\mathbf{p}-\langle\mathbf{p}\rangle}{\Lambda}\right]^2}. \tag{5.3}$$

The two potentials $U_1(\rho,\mathbf{p})$ and $U_2(\rho,\mathbf{p})$ can give significantly different results in the following physical situation. Consider two large nuclei which overlap in configuration space but which are disjoint in momentum space (see Fig. 6). One nucleus has nucleon momenta up to p_F centered around $\mathbf{P}_0/2$ and the other around $-\mathbf{P}_0/2$. A typical value of P_0 is 0.8 GeV/c. The potential $U_2(\rho,\mathbf{p})$ depends on the deviation of $\mathbf{p}$ from the average value; this average value is zero. Thus $|\mathbf{p}-\langle\mathbf{p}\rangle|\cong P_0/2$ is large and hence the magnitude of $U_2(\rho,\mathbf{p})$ is considerably weakened. If instead one uses $U_1(\rho,\mathbf{p})$, the nucleon whose momentum is in the first Fermi sphere gets significant contributions from nucleons

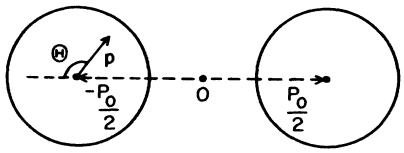

FIG. 6. The two colliding ions as seen in momentum space. Θ is the angle between the momentum $\mathbf{p}$ of a nucleon inside the target and $-\mathbf{P}_0$, where P_0 is the relative momentum.

in the same Fermi sphere although the contribution from the other Fermi sphere is small. The net result for large P_0 is that U_2 becomes less attractive than U_1 while both give comparable values in the local equilibrium situation. This is shown in Figs. 7 and 8. We have also verified that both U_1 and U_2 are consistent with results obtained using the Gogny interaction when local equilibrium prevails.

We have therefore opted to choose a potential energy density which is given by

$$V(\rho)=\frac{A}{2}\frac{\rho^2}{\rho_0}+\frac{B}{\sigma+1}\frac{\rho^{\sigma+1}}{\rho_0^{\sigma}}$$

$$+\frac{C}{\rho_0}\int\int d^3pd^3p' \frac{f(\mathbf{r},\mathbf{p})f(\mathbf{r},\mathbf{p}')}{1+\left[\frac{\mathbf{p}-\mathbf{p}'}{\Lambda}\right]^2}. \tag{5.4}$$

This leads to a potential

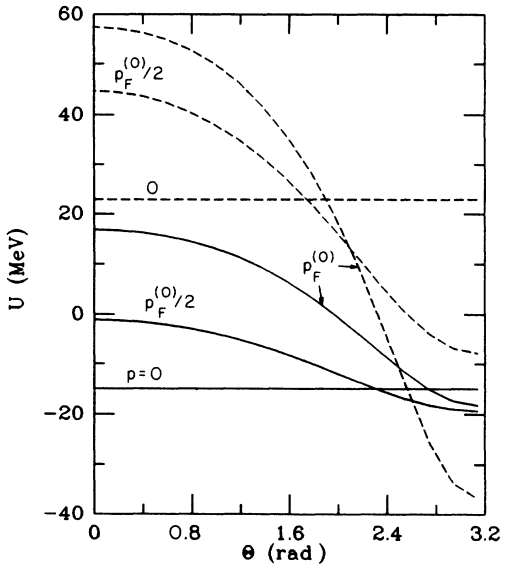

FIG. 7. The single particle potential felt by a nucleon inside one of two separate Fermi fluids overlapping in coordinate space. Θ is defined in Fig. 6. Results are shown for different values of nucleons momentum $\mathbf{p}$ (with $p_F^{(0)}\cong 263$ MeV/c) for the GBD interaction (dashed curves) and the interaction in Eq. (5.5) of the present work (solid curves).

$$U(\rho,\mathbf{p})=A\left[\frac{\rho}{\rho_0}\right]+B\left[\frac{\rho}{\rho_0}\right]^{\sigma}+2\frac{C}{\rho_0}\int d^3p'\frac{f(\mathbf{r},\mathbf{p}')}{1+\left[\frac{\mathbf{p}-\mathbf{p}'}{\Lambda}\right]^2}. \quad (5.5)$$

The advantage of this functional form for momentum dependence is that for cold nuclear matter $[f(\mathbf{r},\mathbf{p})=(4/h^3)\theta(p_F-p)]$ the integrals appearing in Eqs. (5.4) and (5.5) have closed analytical expressions although they are not simple. For completeness we write down the expressions.

$$\int_0^{p_F}\int_0^{p_F}\frac{d^3p\,d^3p'}{1+\left[\frac{\mathbf{p}-\mathbf{p}'}{\Lambda}\right]^2}=\frac{32\pi^2}{3}p_F^4\Lambda^2\left[\tfrac{3}{8}-\frac{\Lambda}{2p_F}\arctan\frac{2p_F}{\Lambda}-\frac{\Lambda^2}{16p_F^2}+\left[\frac{3}{16}\frac{\Lambda^2}{p_F^2}+\frac{1}{64}\frac{\Lambda^4}{p_F^4}\right]\ln\left[1+\frac{4p_F^2}{\Lambda^2}\right]\right], \quad (5.6)$$

$$\int_0^{p_F}\frac{d^3p'}{1+\left[\frac{\mathbf{p}-\mathbf{p}'}{\Lambda}\right]^2}=\pi\Lambda^3\left[\frac{p_F^2+\Lambda^2-p^2}{2p\Lambda}\ln\frac{(p+p_F)^2+\Lambda^2}{(p-p_F)^2+\Lambda^2}+\frac{2p_F}{\Lambda}-2\left[\arctan\frac{p+p_F}{\Lambda}-\arctan\frac{p-p_F}{\Lambda}\right]\right]. \quad (5.7)$$

There are five constants in Eq. (5.4); these are found by requiring that $E/A=-16$ MeV, $\rho_0=0.16$ fm^{-3}, $K=215$ MeV, $U(\rho_0,p=0)=-75$ MeV, and $U[\rho_0,p^2/(2m)=300$ MeV$]=0$. Their values are then $A=-110.44$ MeV, $B=140.9$ MeV, $C=-64.95$ MeV, $\sigma=1.24$ and $\Lambda=1.58p_F^{(0)}$, and yield an effective mass $m^*=0.67m$. With these parameters the new potential of Eq. (5.5) becomes repulsive for cold nuclear matter at normal density for kinetic energy E greater than 300 MeV. For much higher kinetic energies, the potential reaches an asymptotic value of 30.5 MeV. These features are in accord with optical model potential fits to nucleon-nucleus scattering. In contrast, the GBD potential gives an asymptotic value of -1.34 MeV while the Gogny potential gives -8.2 MeV. Thus at high energies the potential in Eq. (5.5) is more repulsive than either the Gogny or the GBD potentials. On the other hand, for reasons explained earlier, this potential can be more attractive than GBD in nonequilibrium situations (see Figs. 7 and 8). Thus it is not obvious how the observables will change compared to the GBD results shown in Fig. 3. The angular distribution calculated with the new momentum dependent interaction Eq. (5.5) is shown in Fig. 9. We find the peak to valley ratio $\mathcal{R}$ to be 4.3 (see Table I). We have checked that the GBD results of Ref. 16 (for Nb on Nb at $E_{\rm lab}/A=400$ MeV with $0<b<3$ fm) change very little if the new interaction Eq. (5.5) is used.

We have also performed a calculation with a hard equation of state using the momentum dependence in Eq. (5.5). We use $K=380$ MeV; the parameters for Eq. (5.5) now are $A=-5.89$ MeV, $B=36.21$ MeV, $C=-64.91$ MeV, $\sigma=2.45$ and $\Lambda=1.58p_F^{(0)}$. This leads to a very large value of $\mathcal{R}=7.4$ (see Table I).

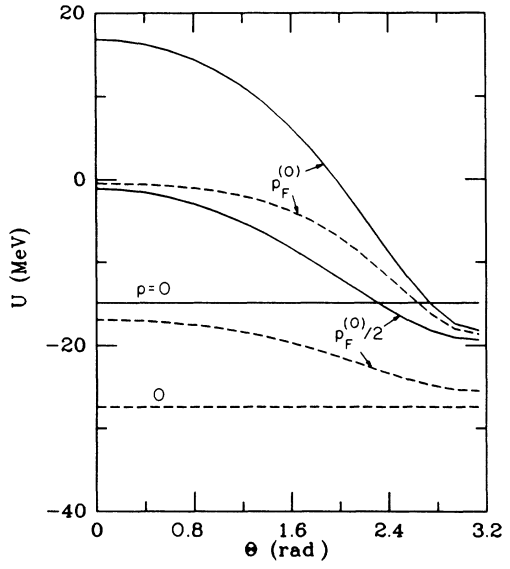

FIG. 8. Same as in Fig. 7, but for the Gogny interaction (dashed curves) and the interaction in Eq. (5.5) of the present work (solid curves).

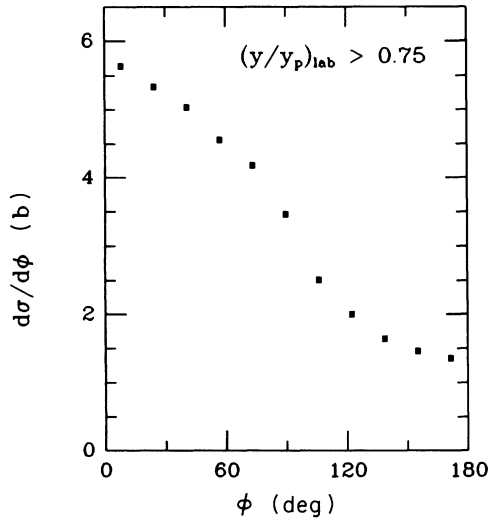

FIG. 9. Same as in Fig. 1, but with the momentum dependent interaction in Eq. (5.5) of the present work.

A recent calculation includes momentum dependence from the Gogny interaction[21] which is suitable for both equilibrium and nonequilibrium situations. The only shortcoming may be that the Gogny potential does not turn repulsive at high momentum, a feature that is demanded by optical model potential fits to nucleon-nucleus scattering.

VI. CONCLUSIONS

We have shown that the ratio of $(d\sigma/d\phi)_{0^\circ}/(d\sigma/d\phi)_{180^\circ}$ for Nb on Nb collisions at 650 MeV/nucleon is a useful probe of the nuclear equation of state. For the cuts employed in this calculation we expect this ratio to be between 3.8 and 4.7. The limits could be narrowed if in-medium cross sections were better determined, perhaps by measurements of other complementary observables which are influenced by the cross sections, but not by the equation of state. Preliminary calculations done here and elsewhere[22] indicate that $d\sigma/d(\cos\theta)$ in the forward direction ($\theta \simeq 20^\circ$) may be such an observable.

ACKNOWLEDGMENTS

We are very grateful to Prof. R. Madey for keeping us informed of the experimental aspects. C.G. is grateful to Prof. G. E. Brown for a short stay at Stony Brook. S.D.G. acknowledges discussions with Prof. G. F. Bertsch; he also thanks Prof. G. E. Brown for much hospitality and many discussions. G.M.W. acknowledges financial support from the Bradlow Foundation. This work was supported by the Department of Energy under Grant No. DE-FG02-88ER40388.

---

*Permanent address: Physics Department, McGill University, Montreal, Province Quebec, Canada.

[1]R. Stock *et al.*, Phys. Rev. Lett. **49**, 1236 (1982).
[2]B. Schürmann, W. Zwermann, and R. Malfliet, Phys. Rep. **147**, 1 (1987).
[3]H. A. Gustafsson *et al.*, Phys. Rev. Lett. **52**, 1590 (1984).
[4]P. Danielwicz and G. Odyniec, Phys. Lett. **157B**, 146 (1985).
[5]K. G. R. Doss *et al.*, Phys. Rev. Lett. **57**, 302 (1986).
[6]R. Stock, Phys. Rep. **135**, 259 (1986).
[7]H. Stöcker and W. Greiner, Phys. Rep. **137**, 277 (1986).
[8]G. F. Bertsch and S. Das Gupta, Phys. Rep. **160**, 189 (1988).
[9]P. Danielewicz, Warsaw University Report IFT/44/87, 1987.
[10]J. W. Harris *et al.*, in Proceedings of the 8th High Energy Heavy Ion Study, edited by J. W. Harris and G. J. Wozniak, Lawrence Berkeley Report No. LBL-24580, 1988.
[11]R. Madey, private communication.
[12]G. Fai, Wei-ming Zhang, and M. Gyulassy, Phys. Rev. C **36**, 597 (1987).
[13]W. Schimmerling, J. W. Kast, D. Ortendahl, R. Madey, R. A. Cecil, B. D. Anderson, and A. R. Baldwin, Phys. Rev. Lett. **43**, 1985 (1979).
[14]K. H. Kampert, Ph.D. thesis, University of Münster, 1986.
[15]G. F. Bertsch, H. Kruse, and S. Das Gupta, Phys. Rev. C **29**, 673 (1984).
[16]C. Gale, G. F. Bertsch, and S. Das Gupta, Phys. Rev. C **35**, 1666 (1987).
[17]G. F. Bertsch, W. G. Lynch, and M. B. Tsang, Phys. Lett. B **189**, 384 (1987).
[18]G. F. Bertsch, G. E. Brown, V. Koch, and B.-A. Li (unpublished).
[19]M. Prakash, T. T. S. Kuo, and S. Das Gupta, Phys. Rev. C **37**, 2253 (1988).
[20]D. Gogny, in *Nuclear Self Consistent Fields,* edited by G. Ripka and M. Porneuf (North-Holland, Amsterdam, 1975), p. 333.
[21]F. Sebille, G. Royer, C. Gregoire, B. Remaud, and P. Schuck, Grand Accelerateur National d'Ions Lourds Report No. GANIL P 88-03, 1988.
[22]H. H. Gan and S. J. Lee (unpublished).